Serine Protease Mechanism: Structure of an Inhibitory Complex of α-Lytic Protease and a Tightly Bound Peptide Boronic Acid†

Roger Bone,‡ Ashok B. Shenvi,§ Charles A. Kettner,§ and David A. Agard*,‡

Department of Biochemistry & Biophysics and Howard Hughes Medical Institute, University of California, San Francisco, San Francisco, California 94143-0448, and Central Research and Development Department, Experimental Station, E. I. du Pont de Nemours and Company, Inc., Wilmington, Delaware 19898

Received April 17, 1987; Revised Manuscript Received July 24, 1987

ABSTRACT: The structure of the complex formed between α-lytic protease, a serine protease secreted by *Lysobacter enzymogenes*, and *N-tert*-butyloxycarbonylalanylprolylvaline boronic acid (K_i = 0.35 nM) has been studied by X-ray crystallography to a resolution of 2.0 Å. The active-site serine forms a covalent, nearly tetrahedral adduct with the boronic acid moiety of the inhibitor. The complex is stabilized by seven hydrogen bonds between the enzyme and inhibitor with additional stabilization arising from van der Waals interactions between enzyme and inhibitor side chains and the burying of 330 Å^2 of hydrophobic surface area. Hydrogen bonding between Asp-102 and His-57 remains intact in the enzyme–inhibitor complex, and His Nϵ_2 is well positioned to donate its hydrogen to the leaving group. Little change in the positions of protease residues was observed on complex formation (root mean square main chain deviation = 0.13 Å), suggesting that in its native state the enzyme is complementary to tetrahedral reaction intermediates or to the nearly tetrahedral transition state for the reaction.

α-Lytic protease is an extracellular serine protease produced by the soil microorganism *Lysobacter enzymogenes*, apparently to bring about the lysis of microbes and small organisms also found in soil (Whitaker, 1970). The enzyme has been extensively studied as a model serine protease largely because it contains a single histidine residue located at the active site, which has facilitated magnetic resonance investigations of the pK_a values of catalytic residues (Robillard & Shulman, 1974; Bachovchin et al., 1981; Bachovchin & Roberts, 1978; Markley & Ibañez, 1978; Westler, 1980). Kinetic, spectroscopic, and crystallographic evidence suggests that peptide bond hydrolysis is accomplished via the stabilization of a high-energy tetrahedral intermediate formed by the nucleophilic attack of serine 195 on the carbonyl of the scissile bond (Scheme I; Hunkapiller et al., 1976; Kaplan & Whitaker, 1969; Delbaere et al., 1981; Brayer et al., 1979a,b; Fujinaga et al., 1985). Recent magnetic resonance studies of the hydrogen-bonding interactions between residues in the catalytic triad (Asp, His, Ser; Bachovchin, 1986) in native and in pmsf[1]-inactivated α-lytic protease have led to the suggestion that formation of tetrahedral intermediates involves disruption of the hydrogen bond between active-site histidine and aspartate residues. It was proposed that hydrogen-bond disruption would allow the histidine to move into a position more optimal for hydrogen-bond donation to the leaving group of the substrate (Bachovchin, 1986). However, inactivated enzyme in which a covalent bond has been formed between the active-site serine and the sulfonyl group of pmsf is not an ideal model for the tetrahedral intermediate formed during peptide hydrolysis; it can mimic neither interactions between the enzyme and substrate side chains nor all of the hydrogen-bonding interactions that stabilize the transition state.

Recently peptide analogues containing an α-amino boronic acid in the carboxy-terminal position have been synthesized and shown to be among the most powerful reversible inhibitors of serine proteases (Kettner & Shenvi, 1984; Matteson et al., 1981). α-Lytic protease is also strongly inhibited by a specific peptide boronic acid, *N-tert*-butyloxycarbonylalanylprolylvaline boronic acid[1] (Boc-Ala-Pro-Bval, K_i = 0.35 nM), which is bound by the enzyme 6–7 orders of magnitude more tightly than substrates (Kettner et al., unpublished results).[2] An earlier crystallographic investigation of a complex formed between subtilisin and the much less specific benzeneboronic acid showed that the boronic acid moiety of the inhibitor formed a tetrahedral adduct with the active-site serine residue (Scheme I; Matthews et al., 1975). However, it was unknown if this mode of interaction might be precluded in the more

Scheme I

α-LYTIC PROTEASE REACTION MECHANISM

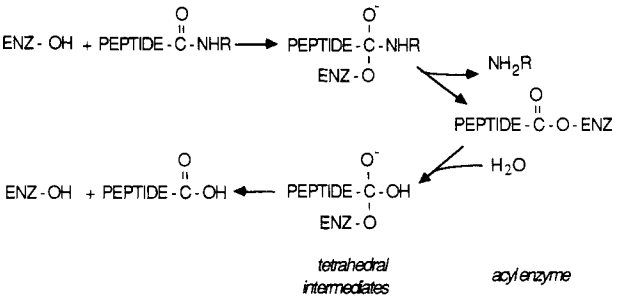

MECHANISM OF PEPTIDE BORONIC ACID INHIBITION

† This work was supported by National Science Foundation Grant DCB8351744 and NIH National Research Service Award GM11174-02.

* Author to whom correspondence should be addressed.
‡ University of California, San Francisco.
§ E. I. du Pont de Nemours and Co.

[1] Abbreviations: Boc, *tert*-butyloxycarbonyl; pmsf, phenylmethanesulfonyl fluoride; rms, root mean square; Tris, tris(hydroxymethyl)-aminomethane; the prefix "boro" indicates that the carboxylic acid moiety (COOH) of the amino acid is replaced by –B(OH)$_2$; valine boronic acid, boroVal, and Bval are used interchangeably. The systematic name for valine boronic acid would be (1-amino-3-methylpropyl)boronic acid.

[2] C. A. Kettner, R. Bone, D. A. Agard, and W. W. Bachovchin, manuscript in preparation.

0006-2960/87/0426-7609$01.50/0

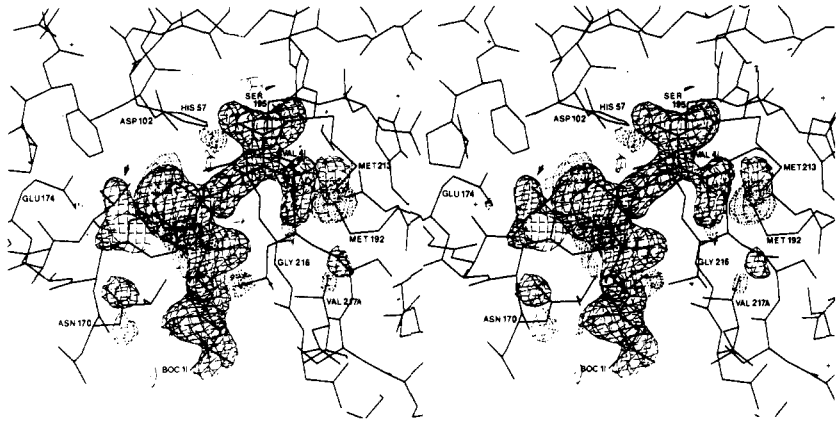

FIGURE 1: Difference electron density map at 2.0-Å resolution of the active-site region of the α-lytic protease complex with Boc-Ala-Pro-Bval (residues 1I–4I). Native α-lytic protease coordinates using chymotrypsin homology numbering, less an active-site sulfate and four waters, and refined inhibitor coordinates are shown. Positive electron density is contoured in dashed lines and negative density in dotted lines.

specific complex of a peptide analogue with the enzyme. Thus the possibility that the peptide boronic acid could form an adduct with the active-site histidine or form a noncovalent complex could not be ruled out (Rawn & Lienhard, 1974).

To understand in greater detail how tetrahedral reaction intermediates are stabilized by the enzyme and whether interaction between the enzyme and these intermediates involves a change in the conformation of the enzyme, we have determined the structure of the complex formed between α-lytic protease and Boc-Ala-Pro-Bval crystallographically to a resolution of 2.0 Å. Of particular interest was whether hydrogen bonding between aspartate and histidine residues in the catalytic triad would be disrupted in the enzyme–inhibitor complex as had been suggested by magnetic resonance studies (Bachovchin, 1986).

Experimental Procedures

α-Lytic protease was purified from culture filtrates of *Lysobacter enzymogenes* 495 and migrated as a single band when electrophoresed on a native polyacrylamide gel at low pH (Whitaker, 1970; Hunkapiller et al., 1973; Hames & Rickwood, 1981). Native crystals were grown by the hanging drop vapor diffusion method (Fehlhammer & Bode, 1975), essentially as described by Brayer et al. (1979b), from unbuffered 1.3 M lithium sulfate at pH 6.8. Single crystals grew after drops had been equilibrated for approximately 10 weeks at ambient temperature. These crystals were used to seed similar unequilibrated droplets that also contained Tris sulfate (20 mM, pH 7.5) to obtain crystals from a buffered solution.

The pinacol ester of Boc-Ala-Pro-Bval, synthesized by established procedures (Kettner & Shenvi, 1984; Matteson et al., 1981) to be described elsewhere (Kettner et al., unpublished results),[2] was dissolved in pH 7.5, 20 mM Tris sulfate at a final concentration of 0.1 M and incubated at room temperature overnight to release the free boronic acid. Single crystals of enzyme–inhibitor complex were obtained either by adding a 1-μL aliquot of 0.1 M boronic acid solution to crystallization drops containing single crystals of α-lytic protease or by seeding unequilibrated drops containing enzyme and inhibitor in a ratio of 1:2. No difference in the rate of crystal growth of seeded native or seeded complex was observed.

Native data (2.4 Å) and enzyme–inhibitor complex data (2.0 Å) were collected from single crystals by using a Syntex $P2_1$ automated diffractometer, equipped with a graphite monochrometer (Stroud et al., 1974; Wycoff et al., 1967). Crystals of enzyme–inhibitor complex were isomorphous with native crystals and had cell parameters that differed by less than 0.15%. The intensities of seven check reflections were monitored in order to correct for crystal decay, which was less than 20% over the course of data collection. Corrections were also made for absorption, Lorentz, and polarization by using standard methods and backgrounds according to Krieger et al. (1974). Data were collected by ω scan in shells of 2θ with the scan rate adjusted so that 90% of the reflections had intensities greater than 3σ over the entire data set (17.5–2.0 Å) with 84% greater than 3σ in the outermost shell (2.25–2.0 Å).

Initial Fourier maps were computed by using refined native α-lytic protease coordinates obtained from M. N. G. James (Fujinaga et al., 1985) with the exception that four water molecules and a sulfate occupying the active site were removed. Maps were inspected and the inhibitor was placed by use of the interactive graphics package FRODO (Jones, 1982) after which the coordinates were refined by the stereochemically restrained least-squares algorithm of Hendrickson and Konnert (1981) as adapted for use on the FPS264 array processor (Furey, 1984) and further modified by us. Surface area calculations were done with the molecular surfacing program MS (Conolly, 1983a,b). The final overall crystallographic R factor for the comparison of observed and calculated structure factors to 2.0 Å was 0.138 with an rms bond deviation of 0.018 Å.

Results

Difference electron density maps clearly showed that the peptide boronic acid is bound to the enzyme at a single site with high occupancy (Figure 1). Maps calculated with Fourier coefficients $(2|F_o| - |F_c|)$ showed continuous electron density stretching between the active-site serine (195 Oγ) and the boronic acid moiety of the inhibitor (Bval 4I, B, Figure 2), strongly suggesting that a covalent adduct had been formed. The covalent nature of the interaction was further supported by the 1.68-Å bond length found on refinement. The geometry of this adduct, based on the shape of the electron density surrounding the boron atom and on the bond angles about the boron after numerous cycles of restrained refinement, is distorted from tetrahedral toward a trigonal planar arrangement[3] with Ser-195 occupying an axial position (Table I). This distorted geometry resulted after refinement with relatively loose restraints (one-fifth of the normal restraints) on the boron–Oγ bond distance and on the boron bond angles. Only when disproportionately tight restraints (5 times the normal

[3] Boron bond angles of 109° would be expected in a purely tetrahedral adduct, while angles of 120° would be expected for a trigonal planar adduct.

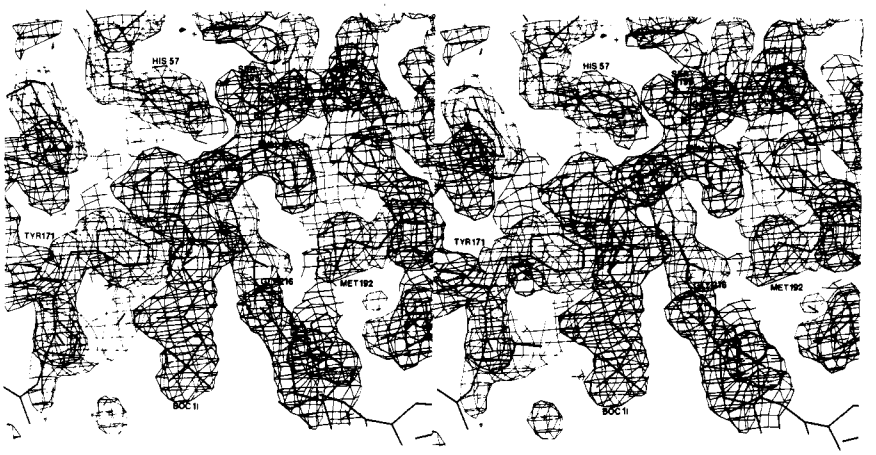

FIGURE 2: Active-site region of the 2.0-Å resolution $2|F_o| - |F_c|$ electron density map with the refined enzyme–inhibitor model and positive density contours. F_c and ϕ_c were calculated from the final refined coordinates of the enzyme–inhibitor complex.

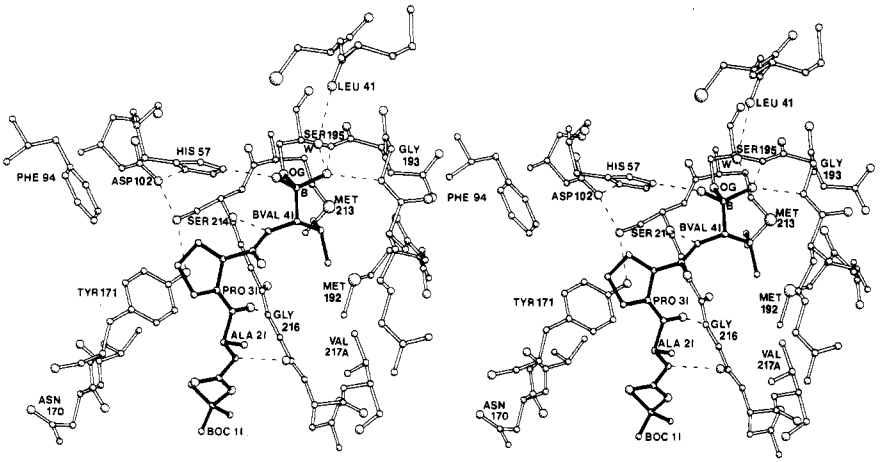

FIGURE 3: Stereo drawing of Boc-Ala-Pro-Bval, residues 1I–4I, in the active site of α-lytic protease. α-Lytic protease in open bonds, inhibitor in filled bonds, and dashed lines for hydrogen bonds. No solvent except water 309 in the complex is shown.

Table I: Geometry of Tetrahedral Boron Adduct

bond	bond length (Å)
Ser-195 Cβ–Ser-195 Oγ	1.45
Ser-195 Oγ–Bval-4I B	1.68
Bval-4I B–Bval-4I O_1	1.52
Bval-4I B–Bval-4I O_2	1.49
Bval-4I B–Bval-4I Cα	1.55
Bval-4I Cα–Bval-4I N	1.48
angle	**bond angle (deg)**
Ser-195 CB–Ser-195 Oγ–Bval-4I B	134.6
Ser-195 Oγ–Bval-4I B–Bval-4I O_1	98.7
Ser-195 Oγ–Bval-4I B–Bval-4I O_2	93.4
Ser-195 Oγ–Bval-4I B–Bval-4I Cα	103.5
Bval-4I O_1–Bval-4I B–Bval-4I O_2	115.3
Bval-4I O_1–Bval-4I B–Bval-4I Cα	116.8
Bval-4I O_2–Bval-4I B–Bval-4I Cα	121.4
Bval-4I B–Bval-4I Cα–Bval-4I N	110.9

Table II: Hydrogen Bonding between α-Lytic Protease and Boc-Ala-Pro-Bval

hydrogen-bonding groups[a]	interatomic distance (Å)
Ser-195 N–Bval-4I O_1	2.9
Gly-193 N–Bval-4I O_1	2.6
His-57 Nϵ_2–Bval-4I O_2	2.7
wat-309 O–Bval-4I O_1	3.3
wat-309 O–Leu-41 O	2.6
wat-292 O–Bval-4I O_2	3.3
wat-292 O–Pro-3I O	2.7
Ser-214 O–Ala-4I N	3.0
Gly-216 N–Ala-2I O	3.0
Gly-216 O–Ala-2I N	2.9
Asp-102 Oδ_1–His-57 Nδ_1	2.8
His-57 Nϵ_2–Ser-195 Oγ	3.0
Asp-102 Oδ_1–His-57 Nδ_1 (native)	2.7
His-57 Nϵ_2–Ser-195 Oγ (native)	3.1

[a] wat = water.

restraints) were used on these parameters could the adduct be forced into a nearly tetrahedral geometry. However, when tight restraints were used, difference maps indicated that the boron should move toward the more planar configuration.

The enzyme–inhibitor adduct is stabilized largely by seven hydrogen bonds between the enzyme, including a tightly bound water molecule (309), and the boronic acid oxygens and between main-chain amide and carbonyl groups on both the enzyme and the inhibitor (Figure 3, Table II). The enzyme amide nitrogens of Ser-195 and Gly-193 comprise the oxyanion binding pocket and form good hydrogen bonds with one of the hydroxyl groups (Bval-4I, O_1) of the boronic acid. In addition, a tightly bound water molecule (309), which forms hydrogen bonds to both the carbonyl of Leu-41 and to another water (259) in the uncomplexed enzyme, moves 0.62 Å in the enzyme–inhibitor complex so that hydrogen bonding can occur with the boronic acid hydroxyl that fills the oxyanion binding pocket. In order to compensate for this movement, water 259 moves 0.18 Å so as to maintain its hydrogen bond with water 309. The other hydroxyl group of the boronic acid (Bval-4I, O_2) forms hydrogen bonds with the imidazole of His-57 and with a water molecule (292) that is also hydrogen bonded to the carbonyl group of the inhibitor proline.

Hydrogen bonds between the amide nitrogen of valine boronic acid (Bval-4I) and the carbonyl of Ser-214, between the

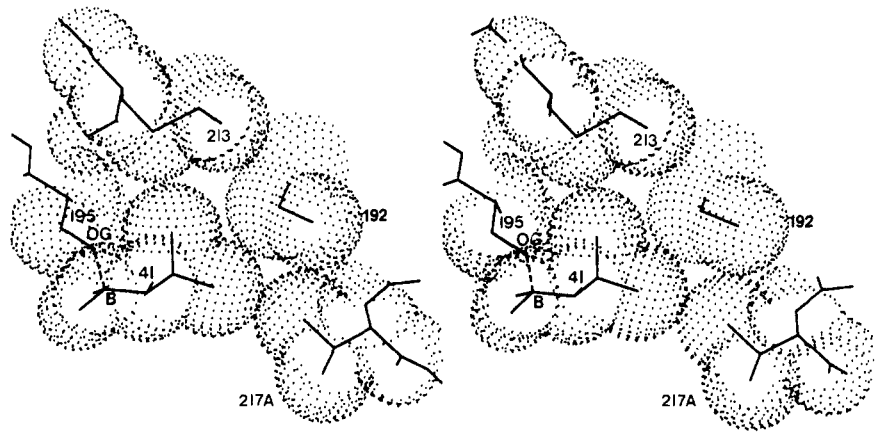

FIGURE 4: Stereo drawing of the P_1 binding site of the enzyme–inhibitor complex with the van der Waals radii of α-lytic protease residues Met-213, Met-192, Val-217A, Ser-195, and inhibitor residue Bval-4I displayed.

amide nitrogen of Gly-216 and the carbonyl of Ala-2I in the inhibitor, and between the amide nitrogen of Ala-2I of the inhibitor and the carbonyl of Gly-216 serve to form an antiparallel β-sheet-like structure between the enzyme and the inhibitor (Figure 3). Five other tightly bound water molecules form a network of hydrogen bonds that cover and hydrogen bond to the solvent-exposed hydrophilic atoms of the inhibitor and enzyme, such as carbonyl groups and the side chain of Arg-192b.

There are three regions of the inhibitor where hydrophobic interactions seem to contribute to the stability of the complex; the total hydrophobic surface area buried on complex formation is approximately 330 Å^2. The valine side chain of the boronic acid residue fits snugly in the P_1 binding site [using the nomenclature of Schecter and Berger (1967)], making very good contacts with the side chains of residues Met-192, Val-217A, and Met-213 (Figure 4). In addition, the subsite is closed over on the top and bottom by the main-chain atoms of residues 214–216 and 191–193. While studies of substrate hydrolysis suggested that an alanyl side chain would be best in this position (Delbaere et al., 1981), studies of boronic acid inhibition showed that valineboronic acid in the P_1 position is 10-fold more effective than the corresponding alanine boronic acid (Kettner et al., unpublished results).[2] In the P_2 site, the prolyl residue of the inhibitor is in an ideal position to pack against the ring of Tyr-171. Additional good contacts can be formed between the proline side chain and the side chains of His-57 and Phe-94. The packing in this region of the complex suggests that substitution of any other residue for the P_2 proline would be deleterious. Indeed, peptide boronic acids containing alanine at this position are bound by a factor of 10 less tightly than those containing proline. Fixation of the main-chain geometry of the inhibitor by a proline in the P_2 position may also contribute to the enhanced affinity.

The butyloxycarbonyl group at the N-terminus of the inhibitor is bound at the edge of the active-site cleft, making contacts with both hydrophobic and hydrophilic residues. Though the fit is not optimal and the average temperature factor (mean B = 25 Å^2) suggests increased motional freedom relative to the rest of the inhibitor, interactions with the butyloxycarbonyl group may be sufficient to exclude much of the solvent that would normally occupy this region of the enzyme and surround this group. Release of water from the enzyme and inhibitor may explain the 20-fold increased affinity of the enzyme for Boc-Ala-Pro-Bval over methylsuccinyl-Ala-Ala-Pro-Bval (Kettner et al., unpublished results).[2]

Difference maps calculated by using structure factors either derived from native data or calculated from the refined structure of uncomplexed α-lytic protease show no significant peaks, except in areas noted below. This indicates that there are few if any significant conformational changes in the protein. Superposition of the coordinates of the native enzyme (Fujinaga et al., 1985) and the refined coordinates of the enzyme–inhibitor complex confirm this observation (Figure 5). The root mean square deviation between main-chain coordinates of the α-lytic protease–inhibitor complex and the main-chain coordinates of the native enzyme is 0.13 Å. The imidazole ring of the active-site histidine residue moves only slightly (rms shift = 0.26 Å) and remains in good position to hydrogen bond to Asp-102. His-57 $N\epsilon_2$ is in nearly optimal position to hydrogen bond to the boronic acid hydroxyl group; it also remains close enough to the γ oxygen of Ser-195 to make a hydrogen bond (Table II), though the geometry is less optimal.

Several small movements of side-chain and main-chain atoms do occur, for the most part involving hydrophilic residues on the surface of the protein and removed from the active site. Three small changes in or above the active site are worth noting. In the P_1 binding site the methyl group of Met-192 appears to rotate approximately 120° in order to reduce steric repulsion from the valine side chain of the inhibitor. The side chain of Val-217A moves toward the inhibitor to optimize its hydrophobic packing (rms side chain shift = 0.77 Å). A larger shift (up to 0.6 Å) occurs in the main-chain atoms of a turn comprised of residues 169–174 in the region of the active site involved in making hydrophobic contacts with the proline and butyloxycarbonyl residues of the inhibitor. The main-chain shift appears to be the result of several interactions including an electronic repulsion between the carbonyl groups of the butyloxycarbonyl residue and Asn-170 and the favorable packing between proline in the inhibitor and Tyr-171. Also, Arg-125 undergoes a large side-chain rotation that allows it to make a salt bridge with Glu-174 on an adjacent molecule in the crystal (note positive density in Figure 1, arrow). This allows the hydrophobic portion of the arginine side chain to pack against the inhibitor proline but pushes Ala-172 away from the active site. Movement of Arg-125 displaces a disordered water molecule (318, B = 46 Å^2) that had been hydrogen bonding to Glu-174. Since the change in conformation of Arg-125 occurs only as a result of inhibitor binding, we interpreted it as reinforcing the movement of residues 169–174 rather than causing the movement.

The mean temperature factor of the complex, including His-57, is reduced by 15% relative to the native structure. Four regions have significantly reduced temperature factors: the side chain of Arg-125, which forms a new salt bridge; the side

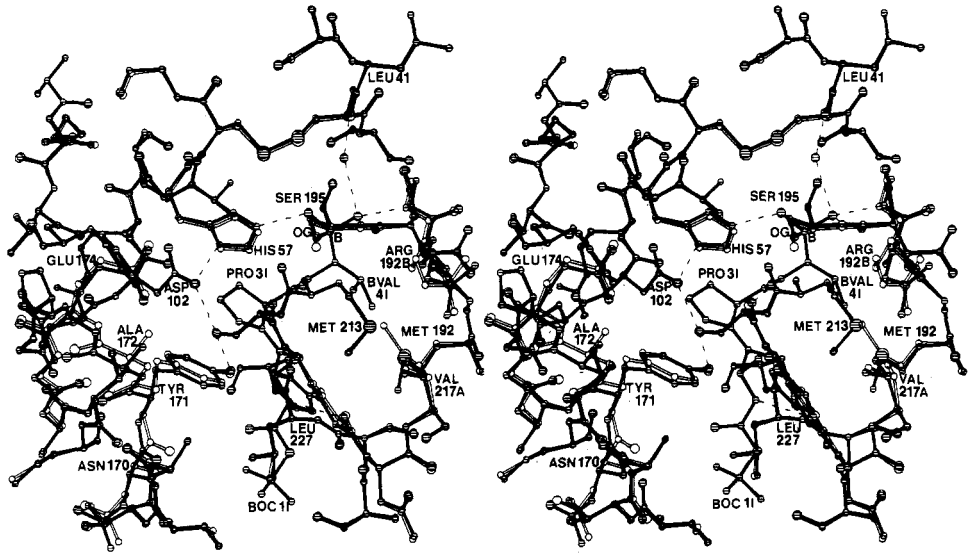

FIGURE 5: Stereo drawing of the active-site region of the complex formed between α-lytic protease and Boc-Ala-Pro-Bval (residues 1I–4I) shown in filled bonds and atoms. Superimposed are the coordinates of uncomplexed α-lytic protease with open bonds and atoms. No solvent except water 309 in the complex is shown.

chain of Arg-192B, whose motion is sterically restrained as a result of inhibitor binding; residues 216 and 217; and residues 169–176. As noted, Glu-174 participates in the new salt bridge with Arg-125 of another molecule in the crystal, while Gly-216, Tyr-171, and Asn-170 are involved in contacts with the inhibitor that have already been described.

Discussion

In the present study it is shown unequivocally that the peptide boronic acid forms a covalent, nearly tetrahedral adduct with the γ oxygen of Ser-195. This result is in accord with previous studies of the weaker complex formed between subtilisin and benzeneboronic acid (Matthews et al., 1975). The structure of the protease–peptide boronic acid complex is also consistent with models of the substrate built into the active site on the basis of the specificity of the enzyme (Delbaere et al., 1981) and with the structure of the complex formed between a homologous protease, *Streptomyces griseus* protease A, and specific peptide aldehyde inhibitors (Brayer et al., 1979a; Delbaere & Brayer, 1985).

The inability of aldehydes to form hydrogen bonds simultaneously to both His-57 and the amide groups in the oxyanion binding site may partially explain why peptide boronic acids are much more effective inhibitors of serine proteases than peptide aldehydes. For instance, acetyl-boroPhe is bound by chymotrypsin 40-fold more strongly than the corresponding aldehyde (Matteson et al., 1981; Chen et al., 1979), succinyl-Ala-Ala-Pro-boroAla is bound to pancreatic elastase over 3 orders of magnitude more strongly than acetyl-Pro-Ala-Pro-alanine aldehyde (Kettner & Shenvi, 1984; Thompson, 1973), and methylsuccinyl-Ala-Ala-Pro-Bval is bound by α-lytic protease nearly 4 orders of magnitude more tightly than the corresponding aldehyde (Kettner et al., unpublished results).[2] The absence of simultaneous hydrogen bonding may also explain the increased temperature factors and conformational changes observed for His-57 in structures of peptide aldehyde complexes with *Streptomyces griseus* protease A (Delbaere et al., 1985; Brayer et al., 1979a). An additional advantage of boronic acid inhibitors might be derived from the negatively charged boron in the tetrahedral adduct interacting favorably with the positively charged His-57.

^{15}N NMR studies have suggested that the hydrogen bond between Asp-102 and His-57 is disrupted when the enzyme reacts with a substrate forming a tetrahedral intermediate

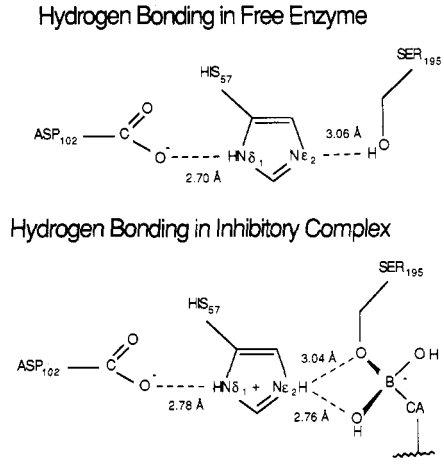

FIGURE 6

(Bachovchin, 1986). It was proposed that this hydrogen-bond disruption would allow His-57 to move into a position optimal for the donation of its proton to the leaving group of the peptide. However, in the structure of the complex between α-lytic protease and Boc-Ala-Pro-Bval, no disruption of the Asp–His hydrogen bond is observed. In this complex, His-57 remains in excellent position to hydrogen bond not only with Asp-102 (His-57, $N\delta_1$–Asp-102, $O\delta_1$ distance = 2.78 Å) but also with one of the hydroxyl groups of the boronic acid (Figure 6). This is accomplished with shifts of 0.2 and 0.3 Å in the positions of the histidine nitrogens $N\delta_1$ and $N\epsilon_2$, respectively (Figure 5) and does not result in increased temperature factors for any of the histidine ring atoms. In addition, in the tetrahedral complex the position of histidine $N\epsilon_2$ appears more optimal for proton donation to the leaving group, as represented by the hydroxyl group of the boronic acid (His-57, $N\epsilon_2$–Bval-4I, O_1, distance = 2.76 Å), than for proton donation back to Ser-195 (His-57, $N\epsilon_2$–Ser-195, Oγ distance = 3.04 Å; see Figure 6). While small shifts in the positions of residues in the catalytic triad appear to have occurred (0.05–0.3 Å) in order to optimize hydrogen bonding in the inhibitory complex, there has been no disruption in the aspartate–histidine hydrogen bond.

The structure of the complex formed between α-lytic protease and Boc-Ala-Pro-Bval appears to be an ideal model for

the structure of tetrahedral reaction intermediates formed during peptide bond hydrolysis. Interactions leading to stabilization of the inhibitory complex (hydrophobic interactions in the P_1 and P_2 binding sites and hydrogen-bond formation with the boronic acid oxygens and peptide carbonyl and amide groups) are presumed to also stabilize the high-energy tetrahedral intermediates on the reaction pathway. Our analysis suggests that stabilization of these intermediates by the enzyme does not require any large changes in the positions of protease residues. These results suggest that α-lytic protease in its native structure is largely complementary either to the high-energy tetrahedral intermediate that is formed during substrate hydrolysis or to the nearly tetrahedral transition state for the reaction. When the substrate binds to the enzyme, it can only maximize the energy of interactions with the enzyme if Ser-195 adds to the carbonyl of the scissile bond and transforms the geometry of the carbonyl group from trigonal to tetrahedral (Wolfenden, 1972; Lienhard, 1973).

While the inhibitor is bound by the enzyme very tightly and appears to be an excellent model of the transition state, interactions between the butyloxycarbonyl group and the enzyme are not optimal. Binding might be improved if the carbonyl group of the butyloxycarbonyl residue, which makes an unfavorable contact with the carbonyl group of Asn-170, could be eliminated or replaced with a hydrogen-bond donor. In addition, the hydrophobic *tert*-butyl moiety is poised on the edge of a small hydrophobic pocket made up of residues Leu-227, Leu-180, Val-167, Ala-169, and Ser-225. An extension of approximately two bond lengths would drop this group into the pocket and might substantially increase the buried hydrophobic surface while improving complementarity. The existence of this binding pocket also suggests that the specificity of α-lytic protease may extent over more residues to accommodate a hydrophobic amino acid in the P_5 or P_6 position.

ACKNOWLEDGMENTS

We gratefully acknowledge Robert M. Stroud for allowing us the use of his diffractometer.

REFERENCES

Bachovchin, W. W. (1986) *Biochemistry 25*, 7751–7759.

Bachovchin, W. W., & Roberts, J. D. (1978) *J. Am. Chem. Soc. 100*, 8041–8097.

Bachovchin, W. W., Kaiser, R., Richards, J. H., & Roberts, J. D. (1981) *Proc. Natl. Acad. Sci. U.S.A. 78*, 7323–7326.

Brayer, G. D., Delbaere, L. T. J., James, M. N. G., Bauer, C. A., & Thompson, R. C. (1979a) *Proc. Natl. Acad. Sci. U.S.A. 76*, 96–100.

Brayer, G. D., Delbaere, T. J., & James, M. N. G. (1979b) *J. Mol. Biol. 131*, 743–775.

Chen, R., Gorenstein, D. G., Kenedy, W. P., Lowe, G., Nurse, D., & Schultz, R. (1979) *Biochemistry 18*, 921–926.

Connolly, M. L. (1983a) *J. Appl. Crystallogr. 16*, 548–558.

Connolly, M. L. (1983b) *Science (Washington, D.C.) 221*, 709–713.

Delbaere, L. T. J., & Brayer, G. D. (1985) *J. Mol. Biol. 183*, 89–103.

Delbaere, L. T. J., Brayer, G. D., & James, M. N. G. (1981) *Eur. J. Biochem. 120*, 289–294.

Fehlhammer, H., & Bode, W. (1975) *J. Mol. Biol. 98*, 683–692.

Fujinaga, M., Delbaere, L. T. J., Brayer, G. D., & James, M. N. G. (1985) *J. Mol. Biol. 183*, 479–502.

Furey, W. J. (1984) in *Methods and Applications in Crystallographic Computing* (Hall, S. R., & Ashida, T., Eds.) pp 353–371, Clarendon, Oxford, U.K.

Hames, B. D., & Rickwood, D., Eds. (1981) *Gel Electrophoresis of Proteins*, IRL, Oxford, England.

Hendrickson, W. A., & Konnert, J. (1981) in *Biomolecular Structure, Function, Conformation, and Evolution* (Srinivasan, R., Ed.) Vol. 1, pp 43–47, Pergamon, Oxford, U.K.

Hunkapiller, M. W., Smallcombe, S. H., Whitaker, D. R., & Richards, J. H. (1973) *Biochemistry 12*, 4732–4743.

Hunkapiller, M. W., Forgac, M. D., & Richards, J. H. (1976) *Biochemistry 15*, 5581–5588.

Jones, T. A. (1982) in *Computational Crystallography* (Sayre, D., Ed.) pp 303–317, Oxford University, Oxford, England.

Kaplan, H., & Whitaker, D. R. (1969) *Can. J. Biochem. 47*, 305–316.

Kettner, C. A., & Shenvi, A. B. (1984) *J. Biol. Chem. 259*, 15106–15114.

Krieger, M., Chambers, J. L., Christoph, G. G., & Stroud, R. M. (1974) *Acta Crystallogr., Sect. A: Cryst. Phys., Diffr., Theor. Gen. Crystallogr. A30*, 740–748.

Lienhard, G. E. (1973) *Science (Washington, D.C.) 180*, 149–154.

Markley, J. L., & Ibañez, I. B. (1978) *Biochemistry 17*, 4627–4640.

Matteson, D. S., Sadhu, K. M., & Lienhard, G. E. (1981) *J. Am. Chem. Soc. 103*, 5241–5242.

Matthews, D. A., Alden, R. A., Birktoft, J. J., Freer, S. T., & Kraut, J. (1975) *J. Biol. Chem. 250*, 7120–7126.

Rawn, J. D., & Lienhard, G. E. (1974) *Biochemistry 13*, 3124–3130.

Robillard, G., & Shulman, R. G. (1974) *J. Mol. Biol. 86*, 541–558.

Schechter, I., & Berger, A. (1967) *Biochem. Biophys. Res. Commun. 27*, 157.

Stroud, R. M., Kieg, L. J., & Dickerson, R. E. (1974) *J. Mol. Biol. 83*, 185.

Thompson, R. C. (1973) *Biochemistry 12*, 47–51.

Westler, W. M. (1980) Ph.D. Dissertation, Purdue University, West Lafayette, IN.

Whitaker, D. R. (1970) *Methods Enzymol. 19*, 599–613.

Wolfenden, R. (1972) *Acc. Chem. Res. 5*, 10–18.

Wyckoff, H. W., Doscher, R., Tsernoglou, D., Inagami, T., Johnson, L., Hardman, K. D., Allewell, N. M., Kelly, D. M., & Richards, F. M. (1967) *J. Mol. Biol. 27*, 563–578.